

# A Programmable Laboratory Testbed in Support of Evaluation of Functional Brain Activation

R. L. Barbour<sup>1,3</sup>, H. L. Graber<sup>1,3</sup>, Y. Xu<sup>1,3</sup>, Y. Pei<sup>3</sup>, C. H. Schmitz<sup>4</sup>, D. S. Pfeil<sup>1</sup>, A. Tyagi<sup>1</sup>,  
R. Andronica<sup>1</sup>, D. C. Lee<sup>2,5</sup>, S.-L. S. Barbour<sup>3</sup>, J. D. Nichols<sup>6</sup>, M. E. Pflieger<sup>6</sup>

Departments of <sup>1</sup>Pathology and <sup>2</sup>Surgery, SUNY Downstate Medical Center, Brooklyn, NY 11203 USA; <sup>3</sup>NIRx Medical Technologies LLC., Glen Head, NY 11545, USA; <sup>4</sup>NIRx Medizintechnik GmbH, Baumbachstr. 17, 13189 Berlin, FRG; <sup>5</sup>Interfaith Medical Center, Brooklyn, NY 11213, USA; <sup>6</sup>Source Signal Imaging Inc., San Diego, CA 92102  
randall.barbour@downstate.edu

**Abstract:** Near infrared spectroscopy and electroencephalography are well suited to explore the brain's response to neuroactivation. We have established a stable, programmable laboratory testbed that provides for experimental measures and analysis of neuroactivation-linked bioelectric and hemodynamic responses.

**OCIS codes:** (350.4800) Optical standards and testing; (130.3120) Integrated optics devices

## Introduction

Near infrared spectroscopy (NIRS) and electrical encephalography (EEG) are complementary sensing technologies with the desirable attributes of inherently compact form factors and sensitivity to the principal hemodynamic and bioelectric phenomenologies, respectively, that are associated with neuroactivation. However, a factor important for the development of functional imaging applications based on either modality (or, ultimately, the two used in combination) is the current lack of experimental systems, analogous to phantoms that are routinely used for evaluation of structural imaging methods, that can be used to quantitatively assess the accuracy of derived functional information. To address this need, we have undertaken a technology integration effort whose principal aims are the ability to: (1) initiate and recover complex macroscopic behaviors that, in general, are not directly observable; (2) implement them in a longitudinally stable, anthropomorphic head form that supports translation from laboratory-based to subject-based studies.

The first aim above is addressed by manufacturing programmable dynamic phantoms for hemodynamic and bioelectric studies. Building on previously reported work [1], our second-generation device has an anthropomorphic form similar to that of the original, but with the added features of a hermitically sealed, conducting brain space that is stabilized against biological degradation. The brain compartment contains programmable source elements—electrochromic cells and electric dipoles—that can be precisely controlled electronically. Manipulation of the voltage across the leads of an electrochromic cell (ECC) changes its opacity, as a way of mimicking time-varying blood volume or oxygen saturation. In similar fashion, the dipoles can be used to model time-varying EEG sources.

The second objective is accomplished by employing the same sensing devices, headgear, and analysis resources as are used in human- or animal-subject studies to explore the programmable validating environment, or Testbed.

## Testbed Components

*Anthropomorphic Dynamic Phantom:* The earlier approach [1] has been extended by introducing into the phantom a “brain” (Fig. 1A) which is composed of a hydrogel-based biopolymer with saline added to mimic impedances typical of real tissue. Commonly available stabilizers are included to inhibit bacterial and mold growth, and TiO<sub>2</sub> and India Ink are added to provide physiologically plausible optical coefficients.

The embedded source array includes two different types of signal-generating arrangements (Fig. 1B). One type features an ECC, dipole and locating LED within an integrated assembly having linear dimensions of ~1.5 cm, to support modeling of induced neural signals and accompanying local hemodynamic responses. In recognition that deep-lying bioelectric sources in the adult brain are detectable by EEG but not by NIRS measurements, the other signal-generating arrangement includes only dipoles positioned at depths of 3-5 cm.

*NIRS-EEG Data Analysis and Mapping Environment:* For processing of NIRS data, we have introduced NAVI [2,3], a MATLAB-based environment that supports many of the principal data transformations common to evaluation of bioelectric and hemodynamic studies, and is geared mainly toward supporting atlas-based parametric mapping with full 3D tomographic capabilities. The package includes modules for image formation, display and analysis; an electronic ledger that automatically records metadata associated with the various data transformation resources; and a number of utilities modeled principally after strategies supported by SPM8 [4,5]: GLM-based parametric mapping of detected hemodynamic response functions; atlas-based mapping of image findings onto identified brain regions, with an automated anatomical labeling (AAL) functionality; and examination of effective

connectivity via strategies such as dynamic causal modeling (DCM) [6].

The data analysis environment also includes the EMSE Suite (ElectroMagnetic Source Estimation, Source Signal Imaging), which comprises software modules for integrating EEG with structural MRI [7]: spatial mapping of sensor positions and MRI co-registration; review of EEG data, with various spatial and temporal filters for treating artifacts; mapping signal-space measures topographically onto the head surface; computing and displaying solutions to the cortical current-density inverse-problem; display of MRI data, with tissue segmentation capabilities; mesh generation based on segmented MRIs; and statistical nonparametric mapping, via randomization of experimental conditions, in either signal space or source space.

A flowchart of the integrated analysis environment is shown in Fig. 2. Dotted arrows indicate the points where structural information and functional features derived from inverse-problem computations will feed back into available forward-problem solvers. This is intended to support development of more computation-intensive algorithms within a domain (e.g., iterative and/or nonlinear image reconstructions), or applications that consider both NIRS and EEG data.

*Atlas-based Mapping:* Solutions to either the NIRS or EEG inverse problem ideally would be based on knowledge of individualized boundary conditions. To support instances where such information is not available, we have implemented an alternative solution wherein a selected atlas is substituted for individual-subject structural information. Using resources available in EMSE, we have generated a series of overlapping regions that support specification of any arbitrary sensor arrangement. Once a sensor arrangement is specified, determination of the associated imaging operators is immediately available. The developed human-head atlas is summarized in Fig. 3. A montage of standard EEG electrode positions is included (Fig. 3A) to guide placement of NIRS optodes. A depiction of functional image data interpolated onto the cortical surface, along with a montage of the corresponding sensor array, is shown in Fig. 3B. The array information also is displayed on the atlas segment selected for image reconstruction, as shown in Fig. 3C.

### Demonstrational Application

The time-varying voltage signals shown in Fig. 4 were used to drive three ECCs of a phantom similar to the one in Fig. 1B. The selected ECCs, embedded in locations corresponding to the right frontal, temporal and occipital cortices, are designated ‘F’, ‘T’ and ‘O’, respectively. The driving functions were derived by numerically solving a mathematical model for the net hemodynamic response (blood volume, in this example) of cortical regions that interact with each other in an effective connectivity network [6].

Steady-state, near infrared time-series data were collected using a large-area sensing array and headgear developed for human-subject studies (NIRx Medical Technologies). The data were pre-processed and images reconstructed using the corresponding NAVI functionalities and the three human-head atlas segments corresponding to the selected head regions. Taking the driving-voltage time series as model functions, the GLM image analysis utility of NAVI was used to identify image pixels whose time-varying reconstructed absorption coefficient values are significantly accounted for by the model functions. The image volumes thereby determined were interpolated onto the brain-atlas cortical surface (Fig. 5), using the NAVI utilities that were developed for identification of activated regions in human-subject images. Finally, volume-averaged image time series from the three colored regions in Fig. 5 were used as input for DCM model-selection computations, with the result that the pattern of connectivity used in generating the Fig. 4 data was preferred over alternative connectivity hypotheses that also were considered.

### References

- [1] R. L. Barbour, R. Ansari, R. Al abdi, H. L. Graber, M. B. Levin, Y. Pei, C. H. Schmitz, and Y. Xu, “Validation of near infrared spectroscopic (NIRS) imaging using programmable phantoms,” Paper 687002 in Design and Performance Validation of Phantoms Used in Conjunction with Optical Measurements of Tissue (Proceedings of SPIE, Vol. 6870), R.J. Nordstrom, Ed. (2008).
- [2] Y. Pei, Z. Wang, and R.L. Barbour, “NAVI: A problem solving environment (PSE) for NIRS data analysis,” Poster No. 685 T-AM at Human Brain Mapping 2006 (Florence, Italy, June 11-15, 2006).
- [3] NIRx fNIRS Analysis Environment User’s guide. Available at: [http://otg.downstate.edu/Publication/NIRxPackage\\_02.pdf](http://otg.downstate.edu/Publication/NIRxPackage_02.pdf).
- [4] W. D. Penny, K. J. Friston, J. T. Ashburner, S. J. Kiebel, and T. E. Nichols, Statistical Parametric Mapping: The Analysis of Functional Brain Images. Academic Press, 2006.
- [5] N. Tzourio-Mazoyer, B. Landeau, D. Papathanassiou, F. Crivello, O. Etard, N. Delcroix, B. Mazoyer, and M. Joliot, “Automated anatomical labeling of activations in SPM using a macroscopic anatomical parcellation of the MNI MRI single-subject brain,” *NeuroImage* **15**, 273-289 (2002).
- [6] K. Friston, “Causal modeling and brain connectivity in functional magnetic resonance imaging,” *PLoS Biology* **7**, 0220-0225 (2009).
- [7] Source Signal Imaging, Inc., EMSE@Suite User Manual, Version 5.4, San Diego, 2011. Available at: <ftp://ftp.sourcesignal.com/manuals/>

This research was support in part by the National Institutes of Health (NIH) under Grants nos. R21NS067278, R42NS050007 and 5R44NS049734; by the Defense Advanced Research Projects Agency under Project no. N66001-10-C-2008; and by the New York State Department of Health.

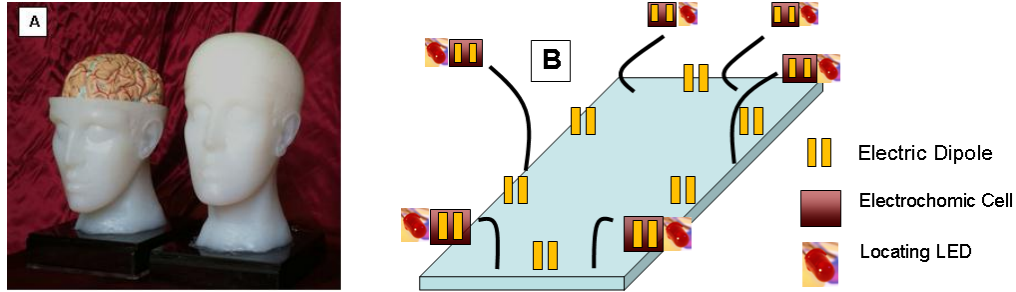


Fig. 1. (A) Partially formed and fully formed head phantom. (B) Schematic of embedded source array containing electric dipoles, ECCs and locating LEDs.

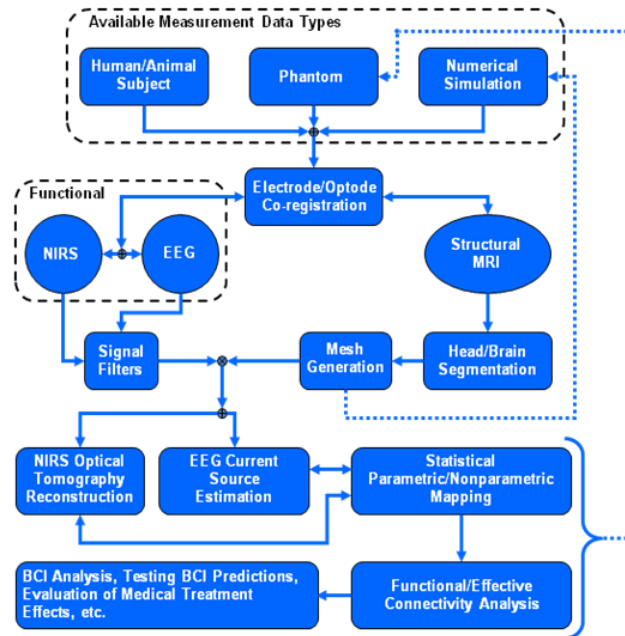


Fig. 2. Flowchart for integrated NIRS/EEG framework. The common anatomical framework is provided by structural MRI.

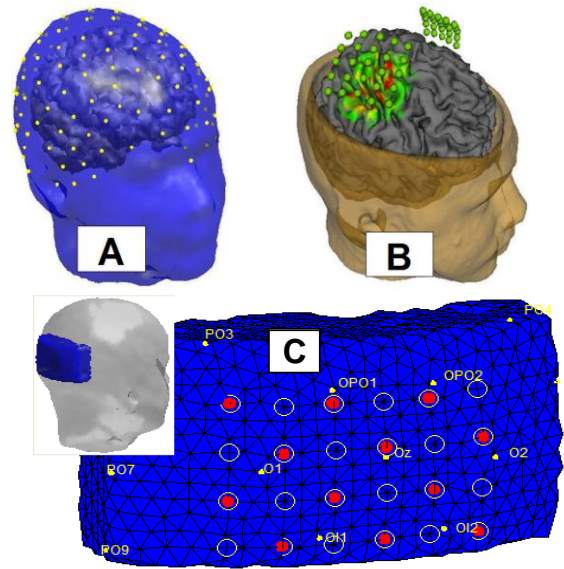


Fig. 3. Graphic summary of the human-head atlas. A, Positions of the EEG electrodes. B, 3D representation of NIRS optode positions and a projection of hemodynamic information onto the cortex. C, Example of an optode sensor array placement, displayed on a selected atlas segment. Open circles = detector fibers; filled circles = detectors co-located with sources; yellow dots = standard EEG electrode locations.

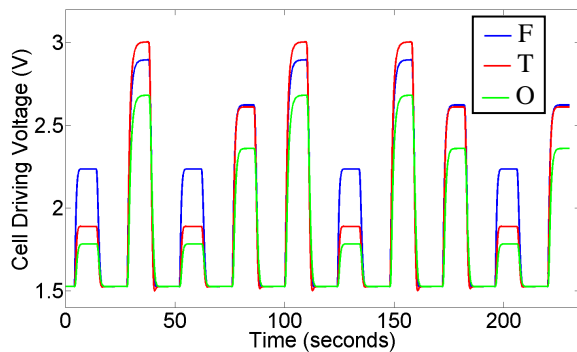


Fig. 4. Time courses of the driving voltages delivered to the ECCs. The plotted functions model the hemodynamic responses of the indicated cortical regions.

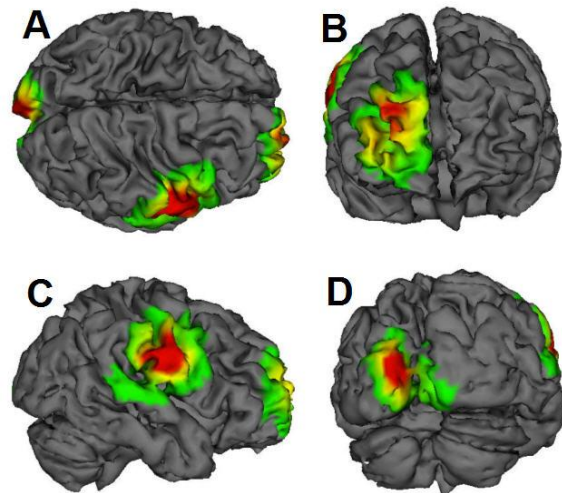


Fig. 5. Cortical surface mapping of GLM coefficients. Plotted quantity (arbitrary units) is the value of the GLM  $\beta$  coefficient obtained by fitting the appropriate ECC driving function to the image time series in each pixel. A - top view, B - frontal view, C - right-side view, D - back view.